Chest Radiograph-based Artificial Intelligence for Osteoporosis
Accuracy and Associations With Fracture and Mortality

Ji Young Lee, MD, PhD, Mi-Sook Kim, PhD, Jinhee Kim, MSc, and Eui Jin Hwang, MD, PhD

Objectives: To evaluate an AI tool for opportunistic osteoporosis screening using chest radiographs (CXRs), focusing on its diagnostic accuracy against dual-energy x-ray absorptiometry (DXA) and associations with long-term risks of fracture and mortality.

Materials and Methods: This retrospective, external validation study included a health checkup cohort with same-day CXR-DXA pairs and a chronic obstructive pulmonary disease (COPD) cohort with available CXRs. We evaluated a commercialized AI tool (InceptionV3 backbone, trained with 55,600 CXR-DXA pairs) designed to identify osteoporosis from a single frontal CXR. Diagnostic performance was assessed against DXA using the area under the receiver operating characteristic curve (AUC). Associations between AI results and subsequent fractures or all-cause mortality were investigated using multivariable Cox proportional-hazard regression, adjusted for sex, age, low body mass index, and COPD stage. Mediation analyses were conducted to examine whether these associations were mediated by a diagnosis of osteoporosis.

Results: In total, 8618 (male-to-female ratio, 2882:5736; mean age, 58 y; median follow-up, 2868 d) and 4941 (male-to-female ratio, 4110:831; mean age, 69 y; median follow-up, 2656 d) patients were included in the health checkup and COPD cohorts, respectively. The AI achieved AUCs of 0.94 (95% CI: 0.93-0.95) and 0.81 (95% CI: 0.76-0.87) for osteoporosis identification in the health checkup and COPD cohorts, respectively. Higher AI-predicted osteoporosis probability was associated with subsequent fracture and mortality in both cohorts ($Ps < 0.05$). Mediation analyses showed that indirect effects of AI scores on fracture or mortality mediated through DXA-defined or clinically diagnosed osteoporosis were not significant ($Ps > 0.05$), suggesting that AI may identify fracture risk in individuals not yet clinically diagnosed with osteoporosis.

Conclusions: AI could identify osteoporosis from chest radiographs, and AI results were associated with subsequent fracture and mortality.

Key Words: osteoporosis, chest radiography, artificial intelligence, deep learning, opportunistic screening, fracture, mortality

(*Invest Radiol* 2026;00:000–000)

Osteoporosis, characterized by reduced bone mineral density (BMD) and microarchitectural deterioration, poses a significant global health burden.[1] It predisposes individuals to fragility fractures, which can lead to chronic pain, disability, reduced quality of life, and increased mortality.[2–4] Early identification is therefore paramount to prevent adverse outcomes.

Currently, the diagnosis of osteoporosis primarily relies on dual-energy x-ray absorptiometry (DXA), while equipment costs, radiation exposure, and the need for specialized technicians limit its accessibility.[2] Consequently, a substantial proportion of at-risk individuals remain undiagnosed. Among Medicare beneficiaries aged > 65 years, BMD assessment using DXA was performed in only 30% of women and 4% of men.[5] Furthermore, before experiencing a fragility fracture, only 10.2% of women and 6% of men underwent BMD testing.[4]

Chest radiography (CXR) is the most frequently performed imaging modality.[6] Given its widespread availability and routine inclusion of the thoracic skeleton, CXR-based assessment presents a compelling opportunity for opportunistic osteoporosis screening. Several studies have demonstrated the feasibility of identifying osteoporosis using AI analysis of CXRs,[7–13] with a recent meta-analysis reporting pooled sensitivity of 0.85 and specificity of 0.83.[14] A recent randomized controlled trial also showed that directing DXA screening to high-risk individuals identified by AI-enabled CXRs improves the detection of osteoporosis.[7] However, the association with long-term outcomes, such as fracture and mortality, has not been sufficiently investigated.

In this study, we externally validated a previously developed deep learning–based AI for the identification of osteoporosis from CXRs,[15] evaluating its accuracy against DXA as well as its association with long-term risks of fractures and mortality in 2 consecutive cohorts of asymptomatic adults undergoing health checkups and patients with chronic obstructive pulmonary disease (COPD). We hypothesized that the AI could identify osteoporosis from CXRs in both cohorts, and the AI analysis results would be associated with subsequent fracture and mortality.

MATERIALS AND METHODS

This single-center, retrospective study was approved by the Institutional Review Board of Seoul National University Hospital (approval number: 2308-141-1459), and the requirement for written informed consent was waived.

Received for publication May 7, 2026; and accepted for publication, after revision, June 19, 2026.

From the Department of Radiology, Seoul National University Hospital and Seoul National University College of Medicine (J.Y.L., E.J.H.); Division of Clinical Epidemiology, Medical Research Collaborating Center, Seoul National University Hospital, Seoul, Republic of Korea (M-.S.K., J.K.).

The chest radiograph datasets analyzed during the current study are not publicly available because of institutional and patient privacy restrictions. De-identified data may be made available from the corresponding author upon reasonable request and with appropriate approvals. The AI software evaluated in this study is a commercially available product, and the trained model weights and source code are not publicly available.

Conflicts of interest and sources of funding: E.J.H. received research grants from Lunit, Coreline Soft, Monitor corporation, Soombit.ai, and Deepnoid outside the present work. Other authors have no conflicts of interest to declare.

Correspondence to: Eui Jin Hwang, MD, PhD, Department of Radiology, Seoul National University Hospital, Seoul National College of Medicine, 101 Daehak-ro, Jongno-gu, Seoul 03080, Korea. E-mail: ken921004@hotmail.com.

Supplemental Digital Content is available for this article. Direct URL citations are provided in the HTML and PDF versions of this article on the journal's website, www.investigativeradiology.com.

ISSN: 1536-0210
DOI: 10.1097/RLI.0000000000001303

Study Population

For this study, we retrospectively collected data from 2 distinct consecutive cohorts: asymptomatic individuals undergoing health checkups (health checkup cohort) and patients diagnosed with COPD (COPD cohort). The health checkup cohort included adults (≥19 y) who underwent erect posteroanterior CXRs and same-day DXA scans from 2014 to 2017. For the COPD cohort, we included adult patients diagnosed with COPD who underwent erect posteroanterior CXRs and pulmonary function tests within a 1-month period between 2011 and 2018 at the same institution (Fig. 1).

Data Collection

All CXRs were obtained in the posteroanterior projection with the patients in an erect position at full inspiration using various ceiling-type fixed radiography scanners.

BMD data were collected using a single DXA scanner (Lunar Prodigy Advance, GE Healthcare). BMD values were measured at the lumbar spine and right proximal femur, and *t*-scores were obtained based on the BMD of young Korean adults aged 20 to 40 years as a reference population. Based on the lowest *t*-score, all results were categorized into 3 categories: osteoporosis (*t*-score ≤−2.5), osteopenia (*t*-score between −2.5 and −1.0), and normal (*t*-score ≥−1.0).[16]

AI Identification of Osteoporosis From CXR

A commercially available AI tool (PROS CXR: OSTEO, Promedius Inc.) was used to analyze the CXRs. This tool was designed to identify the diagnosis of osteoporosis using a single-input frontal CXR. Further information for the development of the AI is described in a previous study[15] and Appendix S1, Supplemental Digital Content 1, http://links.lww.com/RLI/B119. The AI tool provided a probability score (0% to 100%) for each input CXR to have osteoporosis. This tool was approved for clinical use by the Ministry of Food and Drug Safety of Korea.

Accuracy of AI Against DXA

We evaluated the discriminative accuracy of the AI in both cohorts. All CXRs in the health checkup cohort and those with available DXA results within 90 days in the COPD cohort were included in the evaluation. We evaluated the accuracy of AI in identifying individuals with (1) osteoporosis and (2) osteoporosis or osteopenia. We conducted an additional analysis restricted to COPD patients who underwent DXA within 30 days of their CXR.

To evaluate the test-retest reliability of the AI analysis, we included pairs of CXRs obtained within 7 days from the COPD cohort.

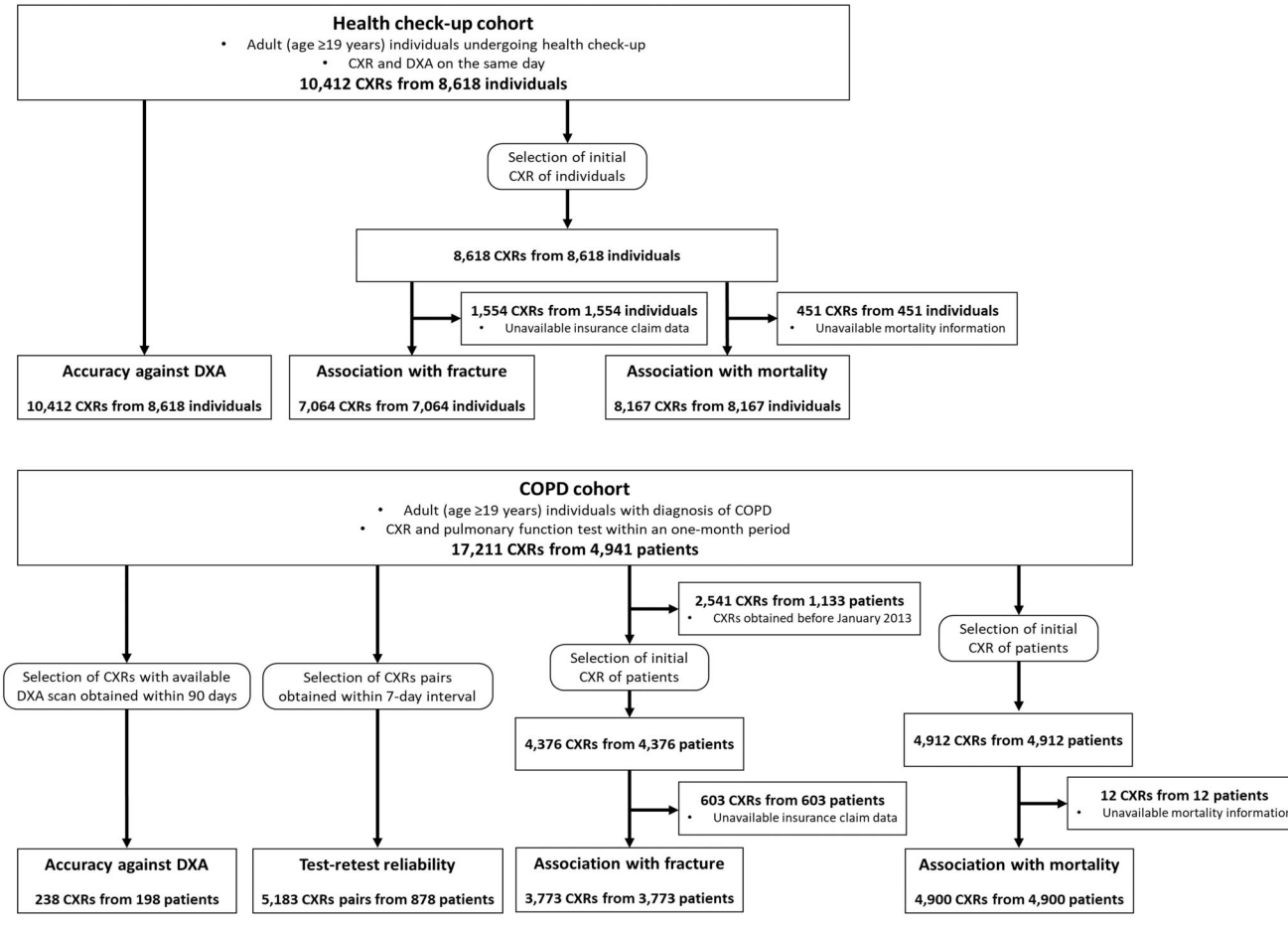

FIGURE 1. Participant flow diagram. COPD, chronic obstructive pulmonary disease; CXR, chest radiograph; DXA, dual-energy x-ray absorptiometry.

Associations With Fracture and Mortality Risk

AI-identified osteoporosis was linked to national insurance claims from 2013 to 2022 and the death registry through December 2023 to identify fractures and all-cause mortality. Fracture occurrence was defined as the first health care claim with a fracture diagnosis recorded after the index CXR. Three claims-based fracture outcomes were evaluated: any-site fracture, hip fracture (proximal femur), and vertebral fracture, with a sensitivity analysis limited to hospitalizations with a fracture diagnosis code. Only the first CXR per individual was analyzed (Appendix S2, Supplemental Digital Content 1, http://links.lww.com/RLI/B119).

Statistical Analysis

The discriminative accuracy of the probability score was evaluated using the area under the receiver operating characteristic curves (AUCs), and compared using the DeLong test. We evaluated sensitivity, specificity, and positive and negative predictive values across multiple probability thresholds. The thresholds of 10%, 20%, and 30% were selected a priori as illustrative operating points to demonstrate performance across a range of sensitivity-specificity tradeoffs and were not intended to represent manufacturer-recommended or clinically validated decision thresholds. The calibration of the AI tool was evaluated using a calibration plot and Spiegelhalter Z-test.[17]

To provide a nonimaging baseline for osteoporosis detection, logistic regression models incorporating age, sex, and body mass index (BMI) were developed. In the COPD cohort, an additional model including Global Initiative for Obstructive Lung Disease (GOLD) stage was evaluated. To assess the incremental value of the AI score beyond clinical variables, combined models incorporating both clinical variables and the AI score were constructed and compared using DeLong's test. Age-stratified and sex-stratified ROC analyses were additionally performed in the health-screening cohort. Furthermore, a guideline-based screening criterion corresponding to women aged 65 years or above, as recommended by the US Preventive Services Task Force,[18] was evaluated and compared with AI-based screening thresholds. To evaluate the clinical utility of the AI probability score, decision curve analysis was performed. The AI score was analyzed both as a continuous variable and as a binary variable using predefined thresholds (10%, 20%, and 30%), and net benefit was compared against treat all and treat none strategies across a range of threshold probabilities. In the COPD cohort, an exploratory subgroup analysis was performed according to COPD severity. Patients were categorized into GOLD stage 1 to 2 and GOLD stage 3 to 4 groups, and the diagnostic performance of the AI model for identifying DXA-defined osteoporosis was evaluated separately in each subgroup.

Test-retest reliability of AI analysis was evaluated using the intraclass correlation coefficient for the continuous score, and using Cohen kappa coefficients for binary results with thresholds of 10%, 20%, and 30%.

For the evaluation of the association between AI analysis and risk of fracture or mortality, we conducted Kaplan-Meier analyses with log-rank tests stratified by threshold probability scores of 10%, 20%, and 30%. Absolute 5-year event risks stratified by AI probability threshold were also estimated. Multivariable Cox proportional hazards regression analyses were conducted to investigate the association between AI-identified osteoporosis and the risk of fracture or mortality. Continuous AI probability scores and binary results with threshold probability scores of 10%, 20%, and 30% were investigated separately as independent variables. Covariates of the analyses included biological sex, age grouped by 10-year intervals, and low BMI (< 18.5 kg/m^2). The age distributions of the fracture and mortality analysis populations are presented in Table S1, Supplemental Digital Content 1, http://links.lww.com/RLI/B119 and the age distributions according to AI-score categories are provided in Table S2, Supplemental Digital Content 1, http://links.lww.com/RLI/B119. The GOLD stage was also regarded as a covariate in the COPD cohort. Model fit was evaluated using Harrell C-index and the likelihood ratio test. The proportional hazard assumption was confirmed using Schoenfeld residuals (all $P > 0.05$).

To investigate whether the association between the AI score and fracture or mortality is mediated by DXA-defined or clinically diagnosed osteoporosis, we conducted mediation analyses. First, in the health checkup cohort, osteoporosis defined by DXA was assessed as a mediator between the AI score and fracture occurrence or all-cause mortality. Subsequently, in both cohorts, we evaluated osteoporosis-naïve individuals to determine whether clinically diagnosed osteoporosis identified via insurance claims following the AI assessment mediated the association between AI scores and subsequent fractures (Appendix S3, Supplemental Digital Content 1, http://links.lww.com/RLI/B119).

To assess whether the AI score adds predictive value for fracture or mortality beyond clinical covariates and DXA-defined osteoporosis, we conducted net reclassification improvement (NRI) analyses using 5-year risk estimates from time-to-event models (Appendix S4, Supplemental Digital Content 1, http://links.lww.com/RLI/B119).

All statistical analyses were performed using SAS Enterprise Guide (version 7.1; SAS Institute Inc.), SPSS (version 29.0; IBM Corp.), and R (version 4.4.1; R Project for Statistical Computing). Statistical significance was set at $P < 0.05$.

RESULTS

Baseline Characteristics

We included 10,412 CXRs from 8618 individuals [5736 women and 2882 men; mean age at initial CXR, 58 y (SD, 9 y)] in the health checkup cohort and 17211 CXRs from 4941 patients [831 women and 4110 men; mean age at initial CXR, 69 years (SD, 10 y)] in the COPD cohort (Table 1).

TABLE 1. Baseline Characteristics of the Participants

Characteristic	Health Checkup Cohort (n = 8618)	COPD Cohort (n = 4941)
Biological sex		
Female	5736 (66.6)	831 (16.8)
Male	2882 (33.4)	4110 (83.2)
Age (y)	58 ± 9	69 ± 11
BMI (kg/m²)	23 ± 3	23 ± 3
Low BMI (< 18.5 kg/m²)	330 (3.8)	444 (9.0)
GOLD stage of COPD		
Stage 1	Not applicable	2365 (47.9)
Stage 2	Not applicable	1898 (38.4)
Stage 3	Not applicable	588 (11.9)
Stage 4	Not applicable	66 (1.3)

Data are reported as mean ± SD, number (percentage)
BMI, body mass index; GOLD, Global Initiative for Obstructive Lung Disease; COPD, chronic obstructive pulmonary disease.

Accuracy of AI Against DXA

All 10,412 CXRs with the same-day DXA scans in the health checkup cohort and 238 CXRs from 198 patients with available DXA scans obtained within 90 days in the COPD cohort were included in the accuracy analyses (Fig. 1).

In the health checkup cohort, 440 (4.3%) and 4385 (42.1%) CXRs were classified as osteoporosis and osteopenia, respectively, by DXA results. For the identification of osteoporosis, the AI tool showed an AUC of 0.94 (95% CI: 0.93-0.95). For the identification of osteoporosis or osteopenia, the AI tool showed an AUC of 0.88 (95% CI: 0.87-0.88) (Fig. 2). Compared with a clinical model incorporating age, sex, and BMI (AUC, 0.78; 95% CI: 0.76-0.80), the AI tool demonstrated significantly higher discrimination for identifying DXA-defined osteoporosis ($P < 0.001$). A combined model incorporating age, sex, BMI, and the AI score achieved an AUC of 0.94 (95% CI: 0.93-0.95), representing a significant improvement over the clinical model alone ($P < 0.001$). In contrast, adding age, sex, and BMI to the AI model did not significantly improve discrimination ($P = 0.401$) (Fig. 3).

In age-stratified and sex-stratified analyses, the AI model maintained excellent discrimination across all subgroups. The AUC was 0.94 (95% CI: 0.93-0.95) among individuals younger than 65 years and 0.91 (95% CI: 0.89-0.92) among those aged 65 years or older. Similarly, the AUC was 0.93 (95% CI: 0.92-0.94) in females and 0.95 (95% CI: 0.93-0.97) in males (Fig. S1, Supplemental Digital Content 1, http://links.lww.com/RLI/B119).

A guideline-based screening criterion reflecting current recommendations for routine osteoporosis screening in women aged 65 years or above demonstrated a sensitivity of 43.6%, specificity of 83.5%, positive predictive value of 10.4%, and negative predictive value of 97.1% for identifying DXA-defined osteoporosis. In comparison, an AI threshold of 30% achieved a sensitivity of 90.0% at a comparable specificity of 83.6%, indicating substantially improved case detection while maintaining a similar false-positive rate.

Decision curve analysis demonstrated that the AI probability score provided clinical utility across a range of threshold probabilities, with positive net benefit over both treat all and treat none strategies. Among the predefined thresholds, the AI threshold of 30% showed the widest range of clinical applicability, maintaining net benefit up to a threshold probability of

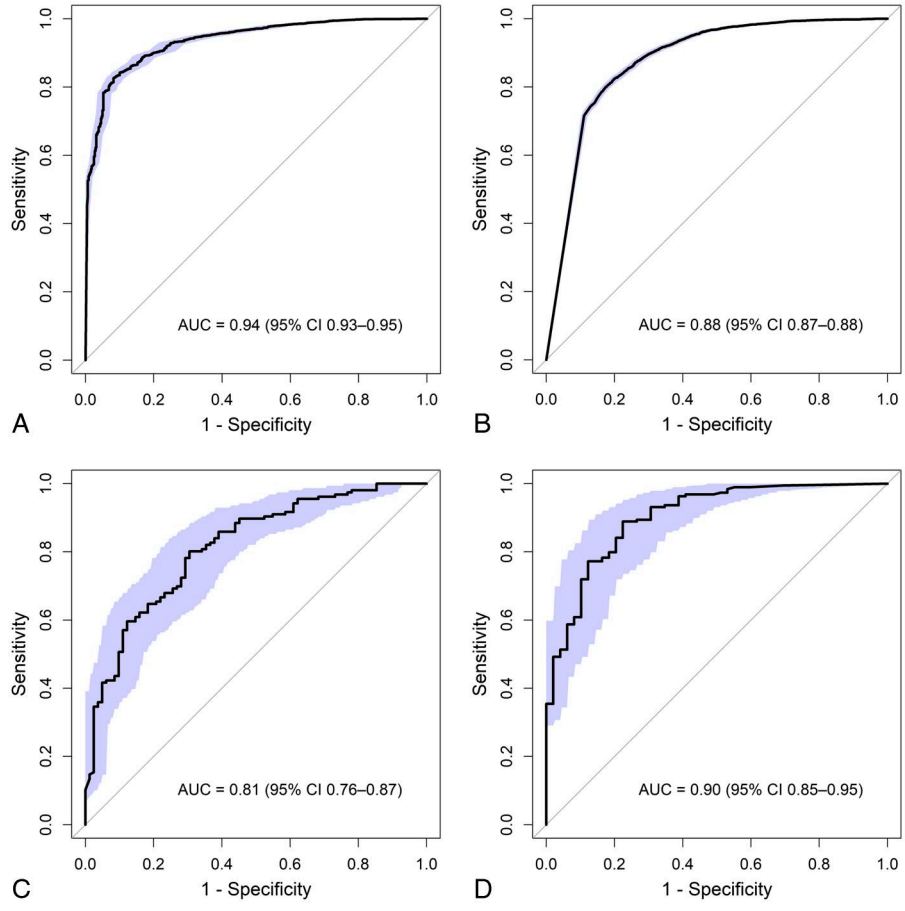

FIGURE 2. Receiver operating characteristic (ROC) curves of the deep learning–based artificial intelligence (AI) tool for the identification of osteoporosis and osteopenia. A, ROC curve for identifying osteoporosis in the health-screening cohort. The area under the curve (AUC) was 0.94 (95% CI: 0.93-0.95). B, ROC curve for identifying osteoporosis or osteopenia in the health-screening cohort. The AUC was 0.88 (95% CI: 0.87-0.88). C, ROC curve for identifying osteoporosis in the chronic obstructive pulmonary disease (COPD) cohort. The AUC was 0.81 (95% CI: 0.76-0.87). D, ROC curves for identifying osteoporosis or osteopenia in the COPD cohort. The AUC was 0.90 (95% CI: 0.85-0.95). AUC, area under receiver operating characteristic curve.

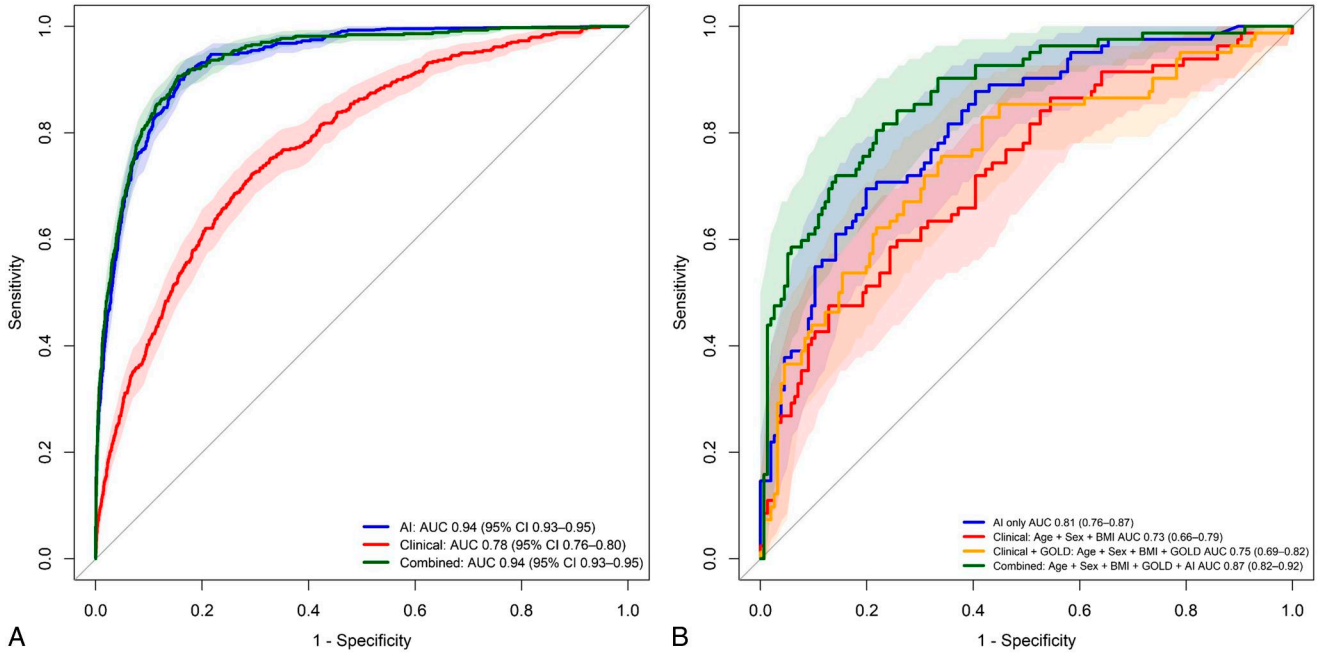

FIGURE 3. Comparison of the diagnostic performance of AI-based, clinical, and combined models for identifying osteoporosis. A, ROC curves of the AI model, clinical model, and combined model in the health-screening cohort. The area under the curve (AUC) was 0.94 (95% CI: 0.93-0.95) for the AI model, 0.78 (95% CI: 0.76-0.80) for the clinical model, and 0.94 (95% CI: 0.93-0.95) for the combined model. B, ROC curves of the AI model, clinical model, clinical model including Global Initiative for Chronic Obstructive Lung Disease (GOLD) stage, and combined model in the COPD cohort. The AUC was 0.81 (95% CI: 0.76-0.87) for the AI model, 0.73 (95% CI: 0.66-0.79) for the clinical model, 0.75 (95% CI: 0.69-0.82) for the clinical model including GOLD stage, and 0.87 (95% CI: 0.82-0.92) for the combined model. AUC, area under receiver operating characteristic curve; GOLD, Global Initiative for Chronic Obstructive Lung Disease.

~22% (Fig. S2, Supplemental Digital Content 1, http://links.lww.com/RLI/B119).

In the COPD cohort, 82 (34.5%) and 107 (45.0%) CXRs were classified as osteoporosis and osteopenia, respectively, by DXA results. The AI tool showed an AUC of 0.81 (95% CI: 0.76-0.87) for the identification of osteoporosis. For the identification of osteoporosis or osteopenia, the AI tool showed an AUC of 0.90 (95% CI: 0.85-0.95) (Fig. 2). A sensitivity analysis restricted to patients who underwent DXA within 30 days of CXR yielded similar results, with AUCs of 0.78 (95% CI: 0.70-0.86) for osteoporosis and 0.87 (95% CI: 0.80-0.94) for osteoporosis or osteopenia, supporting the robustness of the findings despite the temporal interval allowed in the primary analysis (Fig. S3, Supplemental Digital Content 1, http://links.lww.com/RLI/B119). In the COPD cohort, a clinical model incorporating age, sex, and BMI achieved an AUC of 0.73 (95% CI: 0.66-0.79), which increased to 0.75 (95% CI: 0.69-0.82) after inclusion of GOLD stage. A combined model incorporating age, sex, BMI, GOLD stage, and the AI score demonstrated the highest discrimination, with an AUC of 0.87 (95% CI: 0.82-0.92). The combined model significantly outperformed both the clinical model including GOLD stage ($P < 0.001$) and the AI model alone ($P = 0.008$) (Fig. 3). In an exploratory subgroup analysis, the AI model demonstrated an AUC of 0.84 (95% CI: 0.78-0.90) in patients with GOLD stage 1 to 2 disease and 0.73 (95% CI: 0.56-0.91) in those with GOLD stage 3 to 4 disease. Although discrimination tended to be lower in patients with more severe COPD, the difference was not statistically significant ($P = 0.27$) (Fig. S4, Supplemental Digital Content 1, http://links.lww.com/RLI/B119).

The AUCs in the COPD cohort were significantly lower than those in the health checkup cohort (Ps < 0.001, DeLong test). The sensitivity, specificity, and positive and negative predictive values of the AI tool at different probability scores are shown in Table 2. The probability score of the AI tool tended to overestimate the probability of osteoporosis in both the health checkup cohort (calibration slope, 0.892; calibration intercept, −2.354; $P < 0.001$ by Spiegelhalter Z-test) and the COPD cohort (calibration slope, 0.511; calibration intercept, −0.687; $P < 0.001$ by Spiegelhalter Z-test, Fig. 4).

In the test-retest reliability assessment with 5138 pairs of CXRs from 878 COPD patients, the intraclass correlation coefficient of the AI probability score was 0.85 (95% CI: 0.84-0.86). Cohen kappa coefficients at threshold probability scores of 10%, 20%, and 30% were 0.62 (95% CI: 0.60-0.64), 0.69 (95% CI: 0.67-0.71), and 0.72 (95% CI: 0.70-0.74), respectively.

Association With Fracture Risk

To evaluate the subsequent occurrence of fractures, 7064 and 3773 CXRs from unique individuals were included in the health checkup and COPD cohorts, respectively (Fig. 1). In the health checkup cohort, fractures at any site, fractures of the proximal femur, and fractures of the spine occurred in 1270 (18.0%), 65 (0.9%), and 279 (4.0%) individuals, with median overall follow-up durations of 2436 (IQR, 2040 to 2831), 2557 (IQR, 2222 to 2922), and 2526 (IQR, 2191 to 2891) days, respectively. In the Kaplan-Meier analyses, higher probability scores were associated with higher risks for all 3 types of fractures (Ps < 0.001) (Fig. 5 and Fig. S5, Supplemental Digital Content 1, http://links.lww.com/RLI/B119). The 5-year risk of any fracture was 9.55% (95% CI: 8.70%-10.39%) in AI-negative and 19.54% (95% CI: 17.94%-21.11%) in AI-positive individuals at the 10% threshold (Table S3, Supplemental Digital Content 1, http://links.lww.

TABLE 2. Accuracy of the Artificial Intelligence (AI) Tool Against Dual-energy x-ray Absorptiometry

Threshold Probability Score	Osteoporosis by DXA				Osteopenia or Osteoporosis by DXA			
	Sensitivity	Specificity	Positive Predictive Value	Negative Predictive Value	Sensitivity	Specificity	Positive Predictive Value	Negative Predictive Value
Health checkup cohort								
10%	0.96 (423/440)	0.67 (6691/9972)	0.11 (423/3704)	1.00 (6691/6708)	0.67 (3218/4825)	0.91 (5101/5587)	0.87 (3218/3704)	0.76 (5101/6708)
20%	0.95 (417/440)	0.76 (7565/9972)	0.15 (417/2824)	1.00 (7565/7588)	0.54 (2611/4825)	0.96 (5374/5587)	0.92 (2611/2824)	0.71 (5374/7588)
30%	0.90 (396/440)	0.84 (8340/9972)	0.20 (396/2028)	0.99 (8340/8384)	0.40 (1931/4825)	0.98 (5490/5587)	0.95 (1931/2028)	0.65 (5490/8384)
COPD cohort								
10%	0.98 (80/82)	0.35 (54/156)	0.44 (80/182)	0.96 (54/56)	0.89 (169/189)	0.73 (36/49)	0.93 (169/182)	0.64 (36/56)
20%	0.95 (78/82)	0.41 (64/156)	0.46 (78/170)	0.94 (64/68)	0.84 (159/189)	0.78 (38/49)	0.94 (159/170)	0.56 (38/68)
30%	0.90 (74/82)	0.51 (79/156)	0.49 (74/151)	0.91 (79/87)	0.77 (145/189)	0.88 (43/49)	0.96 (145/151)	0.49 (43/87)

Numbers in parentheses indicate numerators/denominators.
COPD, chronic obstructive pulmonary disease; DXA, dual-energy x-ray absorptiometry.

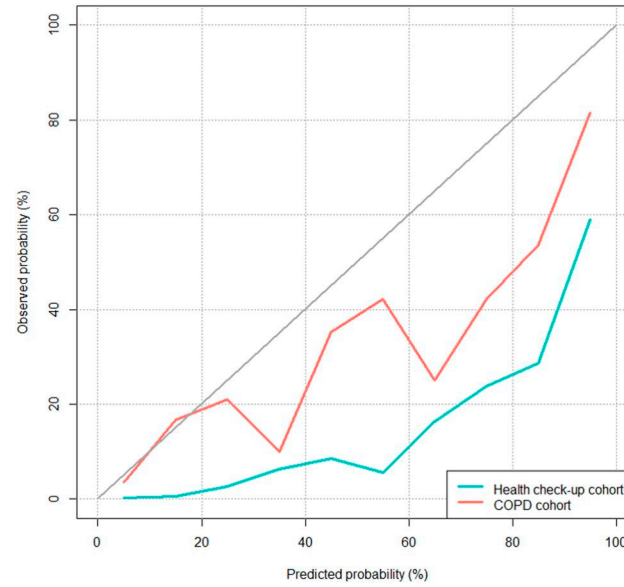

FIGURE 4. Calibration plots for the identification of osteoporosis using the artificial intelligence analysis of chest radiographs. The AI tended to overestimate the probability of osteoporosis in both the health checkup cohort and the chronic obstructive pulmonary disease patient cohort. COPD, chronic obstructive pulmonary disease.

com/RLI/B119). In the Cox proportional hazard regression analyses, higher probability scores were associated with all 3 types of fracture after adjustment of covariates ($Ps \leq 0.045$) (Table 3).

In the COPD cohort, fractures at any site, fractures of the proximal femur, and fractures of the spine occurred in 922 (24.4%), 152 (4.0%), and 338 (9.0%) patients, with median overall follow-up durations of 2710 (IQR, 1918 to 3471), 3044 (IQR, 2252 to 3593), and 2983 (IQR, 2160 to 3562) days, respectively. In the Kaplan-Meier analyses, higher probability scores were associated with higher risks for all 3 types of fractures ($Ps < 0.001$) (Fig. 5 and Fig. S6, Supplemental Digital Content 1, http://links.lww.com/RLI/B119). The 5-year risk of any fracture was 11.52% (95% CI: 9.75%-13.25%) in AI-negative and 20.95% (95% CI: 19.33%-22.54%) in AI-positive patients at the 10% threshold (Table S3, Supplemental Digital Content 1, http://links.lww.com/RLI/B119). In the Cox proportional hazard regression analyses, higher probability scores were associated with all 3 types of fractures after adjusting for covariates ($Ps < 0.001$) (Table 4). The sensitivity analysis with restriction of fracture events to those with hospitalization led to consistent results (Table S4, Supplemental Digital Content 1, http://links.lww.com/RLI/B119).

Mediation analyses showed that indirect effects of AI scores on fractures mediated by DXA-defined osteoporosis were insignificant ($Ps > 0.05$, Table S5, Supplemental Digital Content 1, http://links.lww.com/RLI/B119) in the health checkup cohort. Similarly, in the analysis of osteoporosis-naive individuals, the indirect effect mediated by subsequent clinical diagnosis of osteoporosis was also insignificant ($Ps > 0.05$, Table S6, Supplemental Digital Content 1, http://links.lww.com/RLI/B119).

For 5-year fracture risk, overall risk reclassification improved with the addition of the AI score, with total NRI values ranging from 4.39% to 13.82% in the health checkup cohort and 9.74% to 16.44% in the COPD cohort (Appendix S5,

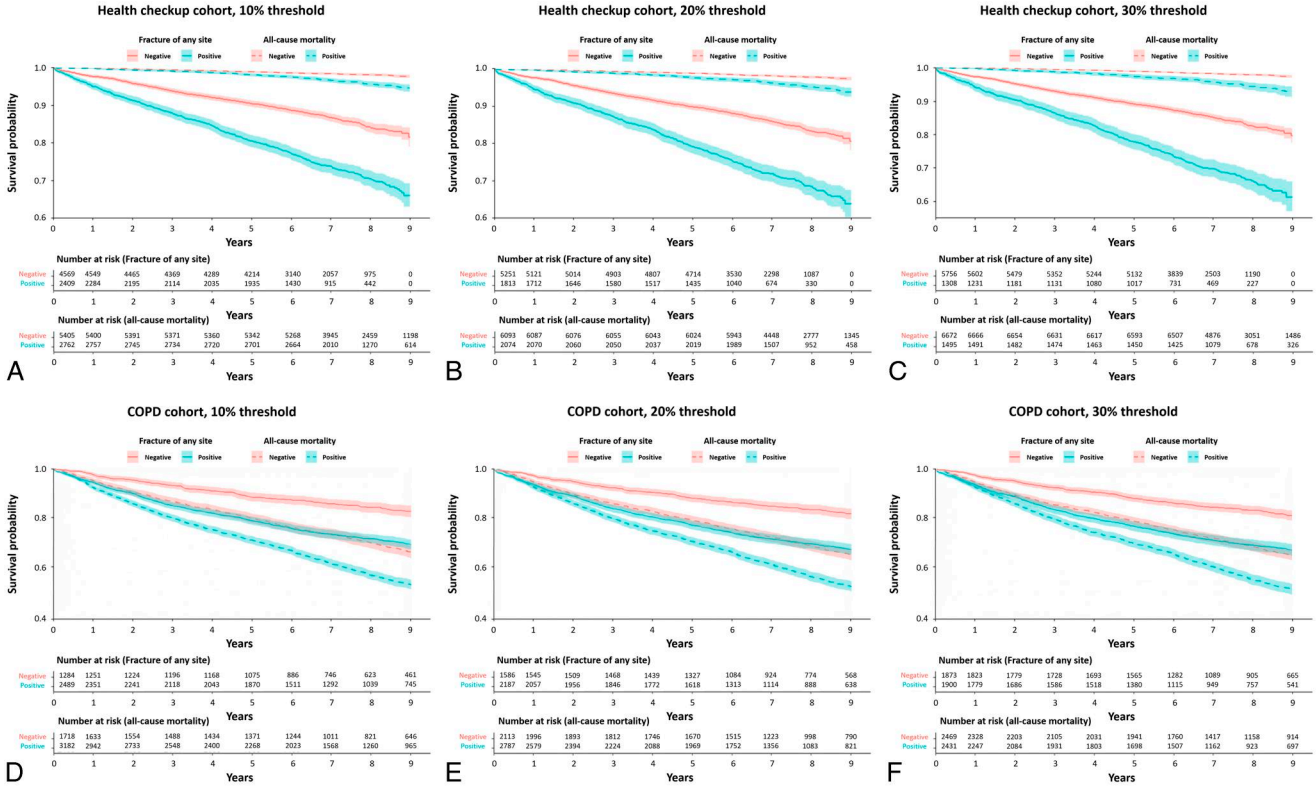

FIGURE 5. Kaplan-Meier curves for time to any-site fracture and all-cause mortality according to AI tool–identified osteoporosis probability scores at different thresholds in the health screening and COPD cohorts. A, Kaplan-Meier curve stratified by a 10% threshold in the health screening cohort. B, Kaplan-Meier curve stratified by a 20% threshold in the health screening cohort. C, Kaplan-Meier curve stratified by a 30% threshold in the health screening cohort. D, Kaplan-Meier curve stratified by a 10% threshold in the COPD cohort. E, Kaplan-Meier curve stratified by a 20% threshold in the COPD cohort. F, Kaplan-Meier curve stratified by a 30% threshold in the COPD cohort.

Tables S7, S8, and S9, Supplemental Digital Content 1, http://links.lww.com/RLI/B119).

Association With Mortality Risk

In the all-cause mortality analyses, 8167 and 4900 CXRs from unique individuals were included in the health checkup and COPD cohorts, respectively (Fig. 1). In the health checkup cohort, 227 (2.8%) deaths were observed, with a median follow-up duration of 2868 (IQR, 2526 to 3228.5) days. Kaplan-Meier analyses revealed that higher probability scores were associated with a higher risk of all-cause mortality ($Ps < 0.001$) (Fig. 5). The 5-year mortality risk was 1.02% (95% CI: 0.75%-1.29%) in AI-negative and 2.10% (95% CI: 1.57%-2.64%) in AI-positive individuals at the 10% threshold (Table S10, Supplemental Digital Content 1, http://links.lww.com/RLI/B119). In the Cox proportional hazard regression analyses, higher probability scores were associated with all-cause mortality after adjusting for covariates ($Ps \le 0.016$) (Table 3).

In the COPD cohort, 2064 (42.1%) deaths were observed, with a median follow-up duration of 2656 (IQR, 1768-3597) days. In the Kaplan-Meier analyses, higher probability scores were associated with a higher risk of all-cause mortality ($Ps < 0.001$) (Fig. 5). The 5-year mortality risk was 20.08% (95% CI: 18.16%-21.95%) in AI-negative and 28.63% (95% CI: 27.04%-30.18%) in AI-positive patients at the 10% threshold (Table S10, Supplemental Digital Content 1, http://links.lww.com/RLI/B119). In the Cox proportional hazard regression analyses, higher probability scores were associated with all-cause mortality after adjusting for covariates ($Ps \le 0.002$) (Table 4).

Sensitivity analyses using continuous age instead of decade-based age categories yielded materially similar results in both cohorts (Table S11, Supplemental Digital Content 1, http://links.lww.com/RLI/B119).

Mediation analyses showed that the indirect effect of AI scores on mortality mediated by DXA-defined osteoporosis was not significant ($Ps > 0.05$, Table S5, Supplemental Digital Content 1, http://links.lww.com/RLI/B119) in the health checkup cohort.

For 5-year all-cause mortality, category-free NRI analyses showed a trend toward reclassification improvements in both cohorts, though more limited than for fracture outcomes (health checkup cohort, 0.20% to 0.33%; COPD cohort, 0.14% to 0.22%) (Table S12, Supplemental Digital Content 1, http://links.lww.com/RLI/B119).

Representative images are presented in Figures 6 and 7.

DISCUSSION

In this study, a deep learning–based artificial intelligence (AI) tool was used to accurately identify individuals with osteoporosis from chest radiographs (CXRs) of asymptomatic individuals undergoing health checkups and patients with chronic obstructive pulmonary disease. Furthermore, AI-identified osteoporosis was associated with subsequent fracture and all-cause mortality in both cohorts. Mediation analyses showed that

TABLE 3. Multivariable Cox Regression Analysis of Fractures and All-cause Mortality in the Health Checkup Cohort

	Fracture of Any Site (n = 7064)				Fracture of proximal femur (n = 7064)				Fracture of spine (n = 7064)				All-cause mortality (n = 8167)			
Independent Variables	Hazard Ratio	*P* for Hazard Ratio	Harrell C-index	*P* for Likelihood Ratio Test*	Hazard Ratio	*P* for Hazard Ratio	Harrell C-index	*P* for Likelihood Ratio Test*	Hazard Ratio	*P* for Hazard Ratio	Harrell C-index	*P* for Likelihood Ratio Test*	Hazard Ratio	*P* for Hazard Ratio	Harrell's C-index	*P* for Likelihood Ratio Test*
Continuous score (per 10% increase)	1.09 (1.07, 1.11)	< 0.001	0.63 (0.61, 0.64)	< 0.001	1.09 (1.00, 1.18)	0.04	0.81 (0.75, 0.86)	< 0.001	1.17 (1.13, 1.22)	< 0.001	0.76 (0.72, 0.79)	< 0.001	1.06 (1.01, 1.11)	0.01	0.75 (0.72, 0.79)	< 0.001
Score ≥10%	1.67 (1.47, 1.88)	< 0.001	0.63 (0.61, 0.64)	< 0.001	1.83 (1.01, 3.29)	0.045	0.80 (0.74, 0.86)	< 0.001	2.48 (1.88, 3.29)	< 0.001	0.75 (0.72, 0.78)	< 0.001	1.52 (1.13, 2.03)	0.005	0.75 (0.72, 0.79)	< 0.001
Score ≥20%	1.66 (1.46, 1.88)	< 0.001	0.62 (0.61, 0.64)	< 0.001	1.94 (1.11, 3.40)	0.02	0.80 (0.75, 0.86)	< .001	2.38 (1.82, 3.11)	< 0.001	0.75 (0.72, 0.78)	< 0.001	1.43 (1.07, 1.92)	0.02	0.75 (0.71, 0.78)	< 0.001
Score ≥30%	1.66 (1.45, 1.89)	< 0.001	0.62 (0.60, 0.63)	< 0.001	1.77 (1.02, 3.05)	0.04	0.80 (0.75, 0.86)	< 0.001	2.44 (1.87, 3.18)	< 0.001	0.75 (0.72, 0.78)	< 0.001	1.62 (1.20, 2.18)	0.002	0.75 (0.72, 0.79)	< 0.001

Covariates of models included biological sex, age grouped by 10 years, and low body mass index (< 18.5 kg/m^2). Numbers in parentheses indicate 95% CIs.
*Comparison with the null model.

TABLE 4. Multivariable Cox Regression Analysis of Fractures and All-cause Mortality in the Chronic Obstructive Pulmonary Disease Cohort

	Fracture of Any Site (n = 3773)				Fracture of Proximal Femur (n = 3773)				Fracture of Spine (n = 3773)				All-cause Mortality (n = 4900)			
Independent Variables	Hazard Ratio	*P* for Hazard Ratio	Harrell's C-index	*P* for Likelihood Ratio Test*	Hazard Ratio	*P* for Hazard Ratio	Harrell's C-index	*P* for Likelihood Ratio Test*	Hazard Ratio	*P* for Hazard Ratio	Harrell C-index	*P* for Likelihood Ratio Test*	Hazard Ratio	*P* for Hazard Ratio	Harrell C-index	*P* for Likelihood Ratio Test*
Continuous score (per 10% increase)	1.12 (1.10, 1.14)	< 0.001	0.64 (0.62, 0.66)	< 0.001	1.16 (1.10, 1.22)	< 0.001	0.73 (0.69, 0.77)	< 0.001	1.21 (1.17, 1.25)	< 0.001	0.73 (0.70, 0.75)	< 0.001	1.02 (1.01, 1.04)	< 0.001	0.68 (0.67, 0.69)	< 0.001
Score ≥10%	1.84 (1.57, 2.16)	< 0.001	0.61 (0.59, 0.63)	< 0.001	2.32 (1.46, 3.69)	< 0.001	0.71 (0.67, 0.75)	< 0.001	3.63 (2.57, 5.13)	< 0.001	0.69 (0.66, 0.72)	< 0.001	1.18 (1.06, 1.30)	0.002	0.68 (0.67, 0.69)	< 0.001
Score ≥20%	1.89 (1.63, 2.20)	< 0.001	0.62 (0.60, 0.64)	< 0.001	2.28 (1.51, 3.44)	< 0.001	0.71 (0.67, 0.76)	< 0.001	3.25 (2.42, 4.37)	< 0.001	0.69 (0.66, 0.72)	< 0.001	1.17 (1.06, 1.28)	0.002	0.68 (0.67, 0.69)	< 0.001
Score ≥30%	1.84 (1.60, 2.12)	< 0.001	0.62 (0.60, 0.64)	< 0.001	2.40 (1.63, 3.53)	< 0.001	0.72 (0.68, 0.76)	< 0.001	3.07 (2.36, 4.01)	< 0.001	0.69 (0.67, 0.72)	< 0.001	1.17 (1.07, 1.29)	< 0.001	0.68 (0.67, 0.69)	< 0.001

Covariates of models included biological sex, age grouped by 10 years, low body mass index (< 18.5 kg/m^2), and Global Initiative for Obstructive Lung Disease stage. Numbers in parentheses indicate 95% CIs.
*Comparison with the null model.

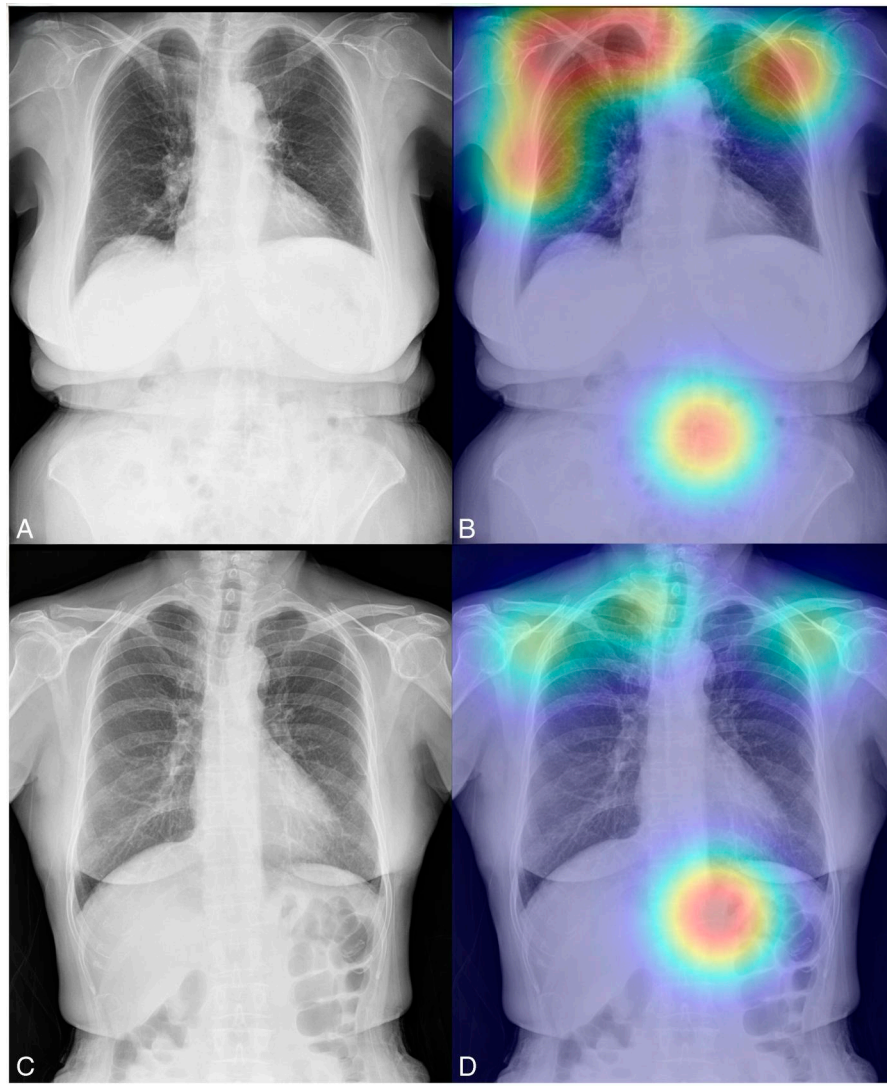

FIGURE 6. Representative cases in which the AI tool assessed the likelihood of osteoporosis from chest radiograph (CXR) with corresponding Gradient-weighted Class Activation Mapping (Grad-CAM) visualizations. A, Chest radiograph of an 84-year-old woman who underwent a routine health checkup. No abnormal findings were observed in either lung field. The AI-identified osteoporosis probability score was 96.54, which corresponded well with a dual-energy x-ray absorptiometry (DXA) *t*-score of −3.3, indicating osteoporosis. B, The accompanying Grad-CAM heatmap illustrates the image regions contributing most strongly to the model's prediction, indicating that areas of bilateral upper ribs and lumbar spine mainly contributed to the prediction of osteoporosis. C, Chest radiograph of a 70-year-old woman who underwent a routine health checkup. No abnormal findings were observed in either lung field. The AI tool assigned an osteoporosis probability score of 0, indicating a low likelihood of osteoporosis. Consistent with this prediction, DXA demonstrated normal bone density with a *t*-score of −0.7. D, The corresponding Grad-CAM heatmap highlights the image regions used by the model in generating its prediction.

the effect of AI prediction had a direct effect on fracture and mortality rather than being indirectly mediated by a diagnosis of osteoporosis. However, the association beyond the known fracture-mortality relationship was not demonstrated.

An important finding of this study is that the AI model provided substantial diagnostic value beyond basic demographic predictors and conventional clinical risk factors. In the health-screening cohort, the AI model significantly outperformed a clinical model based on age, sex, and BMI and maintained excellent discrimination across age and sex subgroups, suggesting that its performance cannot be explained solely by recognition of demographic characteristics. Furthermore, comparison with a guideline-based screening criterion of women aged ≥65 years demonstrated substantially improved case detection at a similar level of specificity. In the COPD cohort, the combination of clinical variables, GOLD stage, and the AI score yielded the highest diagnostic performance, indicating that AI-derived imaging information and conventional clinical predictors provide complementary information for osteoporosis risk assessment.

The accuracy of AI against DXA-defined osteoporosis in the COPD cohort needs to be interpreted with caution due to potential verification bias, as only a subset of COPD patients underwent DXA, likely based on clinical suspicion. This limitation may affect the representativeness of the study population and should be considered when interpreting the results. In

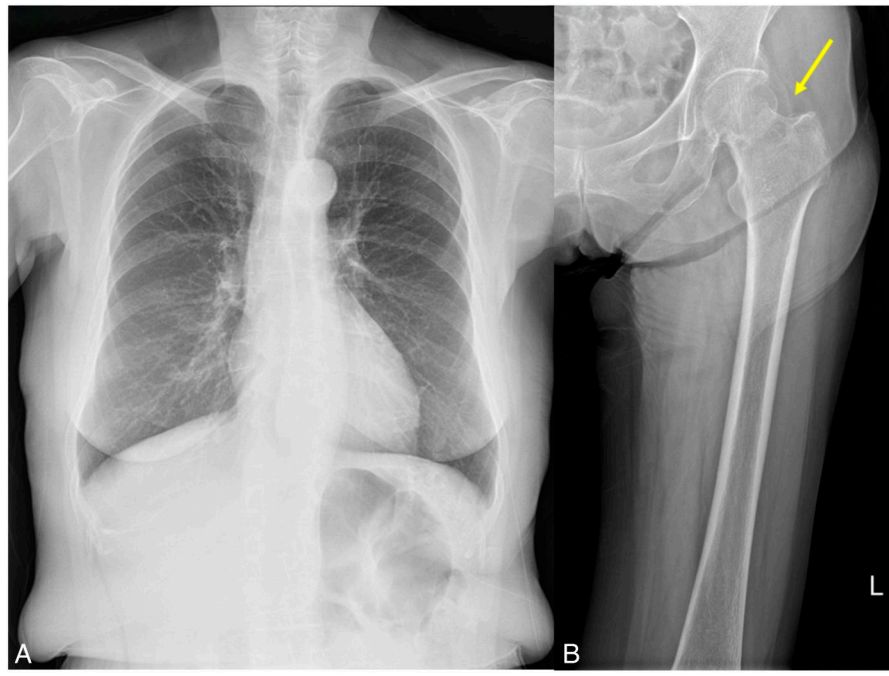

FIGURE 7. Representative case in which the AI tool accurately identified osteoporosis, followed by a subsequent fracture and death. A, Chest radiograph of a 76-year-old woman who had undergone a routine health checkup. No abnormal findings were observed in either lung field. The AI-identified osteoporosis score was 96.12, which corresponded well with a DXA *t*-score of –2.9, indicating accurate identification of osteoporosis. B, A femoral neck fracture (arrow) occurred 5 years later, followed by death one year after the fracture.

addition, DXA was performed within 90 days of CXR in the primary analysis, potentially introducing a temporal mismatch. However, a sensitivity analysis restricted to patients who underwent DXA within 30 days of CXR yielded similar diagnostic performance, suggesting that temporal mismatch had a limited impact on the results. The lower diagnostic accuracy observed in the COPD cohort compared with the health-screening cohort may partly reflect the higher prevalence of radiographic abnormalities in patients with COPD. Supporting this possibility, an exploratory subgroup analysis demonstrated a trend toward lower discrimination in patients with GOLD stage 3 to 4 disease compared with those with GOLD stage 1 to 2 disease, although the difference was not statistically significant. These findings suggest that disease-related factors associated with COPD may influence AI performance and warrant further investigation in larger cohorts. Nevertheless, given the increased risk of secondary osteoporosis in patients with COPD[19,20] and the frequent use of CXRs in this population, AI-enabled opportunistic screening may still provide a practical approach for identifying patients who could benefit from DXA evaluation. In this context, it is notable that the AI maintained similar sensitivity across both cohorts, even though specificity was reduced in the COPD cohort at the same thresholds, suggesting that the model may retain its utility as a screening tool despite the inherent challenges of this patient population.

Mediation analyses suggested that the effects of AI results on fractures and mortality were primarily direct, with non-significant indirect effects through DXA-defined or clinically diagnosed osteoporosis. However, these findings require cautious interpretation, given the susceptibility of observational mediation analysis to unmeasured confounding and model misspecification. Nevertheless, these results raise the possibility that AI may identify fracture risk in individuals not yet clinically diagnosed with osteoporosis. Consistent with this, the reclassification for fracture risk improved with the addition of the AI score beyond DXA-defined osteoporosis, suggesting that AI results have added value for identifying high-risk individuals for fracture compared with DXA-defined osteoporosis alone.

Although higher AI probability scores were significantly associated with mortality and showed a significant direct effect in mediation analysis, whether the effect of AI results extends beyond the known fracture-mortality relationship could not be definitively established. The mediating role of fractures in the association between AI-identified osteoporosis and mortality could not be assessed due to the lack of linked, time-sequenced data. Consistently, reclassification improvement of the mortality risk with the addition of AI results was limited compared with the fracture risk. Our findings align with existing evidence that highlights the link between skeletal fragility, fracture events, and increased mortality risk.[21–24] Fracture-associated mortality can be explained by underlying health factors, including dementia, multiple comorbidities, frailty, physical weakness, and low bone mass.[25–28] Opportunistic CT-based BMD assessment has similarly shown strong associations between low BMD and adverse outcomes across various clinical settings,[29–34] with recent advances including novel photon-counting detector CT further expanding technical approaches for opportunistic BMD quantification.[35] Given this established relationship between osteoporosis, fracture, and mortality, identification of low BMD is clinically relevant for long-term outcomes, and AI-based opportunistic detection from routine CXRs may represent a scalable approach to identifying at-risk individuals.

A recent randomized controlled trial demonstrated that AI analysis of CXRs led to increased referral for DXA and higher rates of osteoporosis diagnosis and treatment,[7] and a real-world

study similarly showed that AI integration into radiology workflow nearly doubled initial DXA assessments with higher diagnostic yield than standard-of-care practice.[12] Furthermore, economic modeling studies have suggested that this approach is cost-effective across multiple countries.[36–39] Our findings extend this by suggesting that AI-enabled CXR analysis may help identify high-risk individuals among those who have not yet undergone DXA, enabling timely diagnosis and treatment that could reduce the long-term risk of fracture and mortality. Although clinically actionable thresholds for AI-guided DXA referral remain to be established, lower thresholds may be preferred for opportunistic screening to maximize sensitivity. In our study, the 10% threshold achieved the highest sensitivity while maintaining reasonable specificity, suggesting potential utility as a trigger for DXA referral, whereas higher thresholds may be appropriate when greater specificity is desired. Furthermore, given the observed overestimation of osteoporosis probability, the AI score should not be interpreted as an absolute estimate of osteoporosis risk. Prospective studies are needed to determine optimal implementation strategies, including threshold selection, and to evaluate the impact of AI-guided screening on DXA referral, treatment initiation, fracture prevention, health care resource utilization, and cost-effectiveness. Multicenter external validation across diverse populations will also be necessary to ensure generalizability, as emphasized by a recent Asia-Pacific expert consensus on AI in osteoporosis screening.[40]

This study has limitations. First, as a retrospective, single-center analysis, it may be subject to selection bias and limited generalizability. Prospective multicenter external validation is warranted to confirm the generalizability of our findings. Second, only a small subset of COPD patients had DXA results, introducing potential verification bias. Third, covariate adjustment was limited due to the limited availability of medical records, precluding a fully independent interpretation of the AI score's prognostic associations. Fourth, the fracture-mortality linkage was unavailable, precluding mediation analysis of fractures on mortality and assessment of competing risks. Fifth, fracture events defined by insurance claim data carry a risk of misclassification. Sixth, detailed scanner-level information was unavailable, precluding evaluation of performance variability across different radiography systems. Finally, the classification of DXA results was based on Korean reference data.

In conclusion, a deep learning–based artificial intelligence (AI) tool could accurately identify osteoporosis from chest radiographs, and AI-identified osteoporosis was associated with an increased risk of fractures and mortality. AI may help identify high-risk individuals, potentially reducing the underdiagnosis of osteoporosis and enabling timely intervention to mitigate long-term adverse outcomes.

ACKNOWLEDGMENTS

The authors thank Gaeun Lee, Junhyeok Park, and Jemyoung Lee from Promedius Inc. for their technical support and information regarding the AI software. Promedius Inc. had no role in study design, data collection, data analysis, data interpretation, manuscript preparation, or the decision to submit the manuscript for publication.

REFERENCES

1. Morin SN, Leslie WD, Schousboe JT. Osteoporosis: a review. *JAMA*. 2025;334:894–907.
2. Compston JE, McClung MR, Leslie WD. Osteoporosis. *Lancet*. 2019; 393:364–376.
3. Clynes MA, Harvey NC, Curtis EM, et al. The epidemiology of osteoporosis. *Br Med Bull*. 2020;133:105–117.
4. Hsieh CI, Zheng K, Lin C, et al. Automated bone mineral density prediction and fracture risk assessment using plain radiographs via deep learning. *Nat Commun*. 2021;12:5472.
5. Curtis JR, Carbone L, Cheng H, et al. Longitudinal trends in use of bone mass measurement among older americans, 1999-2005. *J Bone Miner Res*. 2008;23:1061–1067.
6. Radiation UNSCotEoA. *Sources, Effects and Risks of Ionizing Radiation UNSCEAR 2020/2021 Report*. United Nations; 2022.
7. Lin C, Tsai DJ, Wang CC, et al. Osteoporotic precise screening using chest radiography and artificial neural network: the OPSCAN Randomized Controlled Trial. *Radiology*. 2024;311:e231937.
8. Tsai DJ, Lin C, Lin CS, et al. Artificial intelligence-enabled chest X-ray classifies osteoporosis and identifies mortality risk. *J Med Syst*. 2024;48:12.
9. Tseng SC, Lien CE, Lee CH, et al. Clinical validation of a deep learning-based software for lumbar bone mineral density and T-Score prediction from chest X-ray images. *Diagnostics (Basel)*. 2024;14:1208.
10. Sato Y, Yamamoto N, Inagaki N, et al. Deep learning for bone mineral density and T-score prediction from chest X-rays: a multicenter study. *Biomedicines*. 2022;10:2323.
11. Asamoto T, Takegami Y, Sato Y, et al. External validation of a deep learning model for predicting bone mineral density on chest radiographs. *Arch Osteoporos*. 2024;19:15.
12. Syme CA, Lopes M, Bilbily A, et al. Clinical impact of adopting an AI-driven opportunistic bone health screening software using routine X-ray. *Skeletal Radiol*. 2026;55:1321–1327.
13. Chen SH, Chang RE, Lien CE, et al. Advancing diagnostic equity through artificial intelligence chest radiograph screening for osteoporosis in Asian populations. *NPJ Digit Med*. 2026;9:359.
14. Skaik K, Abdallah JP, Koucheki R, et al. Opportunistic screening for osteoporosis using chest X-rays and deep learning: a systematic review and meta-analysis. *Bone*. 2026;210:117923.
15. Jang M, Kim M, Bae SJ, et al. Opportunistic osteoporosis screening using chest radiographs with deep learning: development and external validation with a cohort dataset. *J Bone Miner Res*. 2022;37:369–377.
16. Dimai HP. Use of dual-energy X-ray absorptiometry (DXA) for diagnosis and fracture risk assessment; WHO-criteria, T- and Z-score, and reference databases. *Bone*. 2017;104:39–43.
17. Spiegelhalter DJ. Probabilistic prediction in patient management and clinical trials. *Stat Med*. 1986;5:421–433.
18. Curry SJ, Krist AH, Owens DK, et al. Screening for osteoporosis to prevent fractures: US Preventive Services Task Force Recommendation Statement. *JAMA*. 2018;319:2521–2531.
19. Nadesalingam K, Kirby D. Bone protection in chronic obstructive pulmonary disease (COPD) patients requiring regular intermittent glucocorticoid therapy. *Clin Med (Lond)*. 2013;13:216.
20. Kanis JA, Stevenson M, McCloskey EV, et al. Glucocorticoid-induced osteoporosis: a systematic review and cost-utility analysis. *Health Technol Assess*. 2007;11iii-iv, ix-xi 1–231.
21. Bliuc D, Nguyen ND, Milch VE, et al. Mortality risk associated with low-trauma osteoporotic fracture and subsequent fracture in men and women. *Jama*. 2009;301:513–521.
22. Ganry O, Baudoin C, Fardellone P, et al. Bone mass density and risk of breast cancer and survival in older women. *Eur J Epidemiol*. 2004;19:785–792.
23. Cai S, Fan J, Zhu L, et al. Bone mineral density and osteoporosis in relation to all-cause and cause-specific mortality in NHANES: A population-based cohort study. *Bone*. 2020;141:115597.
24. Cummings SR, Melton LJ. Epidemiology and outcomes of osteoporotic fractures. *Lancet*. 2002;359:1761–1767.
25. Tosteson AN, Gottlieb DJ, Radley DC, et al. Excess mortality following hip fracture: the role of underlying health status. *Osteoporos Int*. 2007;18: 1463–1472.
26. Kado DM, Duong T, Stone KL, et al. Incident vertebral fractures and mortality in older women: a prospective study. *Osteoporos Int*. 2003;14: 589–594.
27. Ensrud KE, Ewing SK, Taylor BC, et al. Frailty and risk of falls, fracture, and mortality in older women: the study of osteoporotic fractures. *J Gerontol A Biol Sci Med Sci*. 2007;62:744–751.
28. Cawthon PM, Marshall LM, Michael Y, et al. Frailty in older men: prevalence, progression, and relationship with mortality. *J Am Geriatr Soc*. 2007;55:1216–1223.

29. Therkildsen J, Nissen L, Jørgensen HS, et al. Thoracic bone mineral density derived from cardiac CT is associated with greater fracture rate. *Radiology*. 2020;296:499–508.
30. Michalski AS, Besler BA, Burt LA, et al. Opportunistic CT screening predicts individuals at risk of major osteoporotic fracture. *Osteoporos Int*. 2021;32:1639–1649.
31. Reid J, McCrosson M, Tobin J, et al. Opportunistic CT screening demonstrates increased risk for peri-articular fractures in osteoporotic patients. *Orthop Traumatol Surg Res*. 2024;110:103935.
32. Paukovitsch M, Fechner T, Felbel D, et al. Opportunistic computed tomography (CT) assessment of osteoporosis in patients undergoing transcatheter aortic valve replacement (TAVR). *Arch Osteoporos*. 2025;20:100.
33. Li Y, Ye K, Liu S, et al. Deep learning-enhanced opportunistic osteoporosis screening in 100 kV Low-voltage chest CT: a novel way toward bone mineral density measurement and radiation dose reduction. *Acad Radiol*. 2025;32:6812–6822.
34. Wu Y, Yang X, Wang M, et al. Artificial intelligence assisted automatic screening of opportunistic osteoporosis in computed tomography images from different scanners. *Eur Radiol*. 2025;35:2287–2295.
35. Moser LJ, Klambauer K, Diaz Machicado MC, et al. In vivo bone mineral density assessment with spectral localizer radiographs from photon-counting detector CT: prospective comparison with DXA. *Invest Radiol*. 2025;60:535–542.
36. Reginster JY, Schmidmaier R, Alokail M, et al. Cost-effectiveness of opportunistic osteoporosis screening using chest radiographs with deep learning in Germany. *Aging Clin Exp Res*. 2025;37:149.
37. Hiligsmann M, Silverman SL, Reginster JY. Cost-effectiveness of opportunistic osteoporosis screening using chest radiographs with deep learning in the United States. *J Am Coll Radiol*. 2025;22:1346–1356.
38. Reginster JY, Hamasaki T, Fujiwara S, et al. Cost-effectiveness of opportunistic osteoporosis screening using artificial-intelligence assisted chest radiographs in Japan. *Osteoporos Sarcopenia*. 2025;11:127–136.
39. Chandran M, Reginster JY, Kim MY, et al. Clinical and economic impact of deep learning-enhanced opportunistic osteoporosis screening using chest radiographs with and without the osteoporosis self-assessment tool for Asians (OSTA). *Osteoporos Int*. 2026;37:717–726.
40. Huang CF, Fang WH, Chen KH, et al. Consensus statement on the application of artificial intelligence in osteoporosis screening and management: perspectives from the Asia-Pacific region. *Osteoporos Int*. 2026. doi:10.1007/s00198-026-08067-6